Anisotropy of x-ray reflectivity: chemical and structural effects on K-shell excitations in hexagonal BN crystal

2002 J. Phys.: Condens. Matter 14 11643

(http://iopscience.iop.org/0953-8984/14/45/308)

INSTITUTE OF PHYSICS PUBLISHING JOURNAL OF PHYSICS: CONDENSED MATTER

J. Phys.: Condens. Matter **14** (2002) 11643–11654 PII: S0953-8984(02)38153-0

Anisotropy of x-ray reflectivity: chemical and structural effects on K-shell excitations in hexagonal BN crystal

E O Filatova and V A Lukyanov

Institute of Physics, St Petersburg University, St Petersburg, 198904, Russia

Received 13 June 2002
Published 1 November 2002
Online at stacks.iop.org/JPhysCM/14/11643

Abstract

The experimental investigation of the B and N K-reflection spectra using both s-polarized synchrotron radiation and unpolarized radiation for different crystal orientations with respect to the electric field vector $\boldsymbol{E}$ was carried out. The absorption spectra calculated from the reflection spectra using Kramers–Kronig analysis are presented. A strong orientation dependence of both reflection and absorption spectra is exhibited. Analysis of the orientation dependences of the x-ray reflection and absorption spectra near both edges strongly supports a possibility of tracing the role of each excitation canal in the formation of fine structure. The high sensitivity of the reflection spectra fine structure to the vibronic interaction connected with Jahn–Teller distortions as well to the core-hole relaxation is discussed. A very strong dependence of the absolute values of the reflectivity on planar crystal anisotropy was discovered.

1. Introduction

Ultrasoft x-ray reflection spectroscopy is one of the spectroscopic methods for shallow core levels. High sensitivity of the reflection spectra near edge fine structure to the sort of atom arranged in a surface layers of solid states, to their chemical state and to the surrounding atom coordination in conjunction with the angular dependence of the depth of the penetration of the reflected x-ray beam opens additional possibilities of this method in studies of anisotropic structures.

Up to now the question of the influence of the spatial crystal anisotropy on the x-ray reflection has been kept in the shade. The early experimental studies of the interaction of x-ray radiation with h-BN [1–3] show a very strong orientation dependence of x-ray reflectivity and scattering due to crystal orientation with respect to the electric field vector. The aim of this paper is to give a comprehensive analysis of the origin of the orientation dependence of K-shell x-ray reflection (and calculated absorption spectra) near edge structure in the h-BN crystal.

H-BN is a one-axis crystal. In the case of a one-axis crystal the dielectric function tensor is always a diagonal matrix if one of the axes of a system of coordinates is aligned with the

crystallographic axis ($\boldsymbol{c}$ axis) of the crystal. In this case $\varepsilon_{xx} = \varepsilon_{yy}$ is valid. In the case of the polarized radiation the problem is simplified. According to [4] the Fresnel equations for s- and p-linearly polarized radiation are given by

$$R_s = \left| \frac{\sin\theta - (\varepsilon_{xx} - \cos^2\theta)^{1/2}}{\sin\theta + (\varepsilon_{xx} - \cos^2\theta)^{1/2}} \right|^2$$
$$R_p = \left| \frac{(\varepsilon_{yy}\varepsilon_{zz})^{1/2}\sin\theta - (\varepsilon_{zz} - \cos^2\theta)^{1/2}}{(\varepsilon_{yy}\varepsilon_{zz})^{1/2}\sin\theta + (\varepsilon_{zz} - \cos^2\theta)^{1/2}} \right|^2, \tag{1}$$

where the axes x and y of a system of coordinates are located in the plane of the reflecting surface of the crystal and the axes y and z are located in the plane of the scattering. One can see from (1) that with the use of p-polarized radiation the reflection coefficient depends on two components of the dielectric function matrix $\varepsilon_{yy} = \varepsilon_\perp$ and $\varepsilon_{zz} = \varepsilon_\parallel$, that is it depends on two components of electric field vector $\boldsymbol{E}$ (perpendicular and parallel to the $\boldsymbol{c}$ axis of the crystal). When using s-polarized radiation the reflection coefficient is defined by the component of the dielectric function matrix for the direction of the electric field vector $\boldsymbol{E}$, which is perpendicular to the $\boldsymbol{c}$ axis of the crystal ($\varepsilon_{xx} = \varepsilon_\parallel$). By this means we assume that the axes x and y of a coordinate system are located in the plane of the reflecting crystal surface which is perpendicular or parallel to the $\boldsymbol{c}$ axis of the crystal. By turning the crystal the $\boldsymbol{E} \perp \boldsymbol{c}$ and $\boldsymbol{E} \parallel \boldsymbol{c}$ alignments are realized and the orientation dependence of the reflection and absorption spectra can be investigated. The greatest effects would be expected when polarized radiation is used, especially in the case of s-polarized radiation; however, these effects have to exist in the reflection spectra of unpolarized radiation.

In this paper we have focused on the consideration of an added bonus that spectroscopy of the mirror reflection and scattering opens for the anisotropic crystal investigation. The results obtained with both s-polarized and unpolarized radiation are discussed and compared. Analysis of B and N K-reflection spectra obtained for different grazing incidence angles and for different crystal orientations with respect to the electric field vector $\boldsymbol{E}$ is carried out. The absorption spectra calculated from reflection spectra using Kramers–Kronig analysis are presented. The high sensitivity of the reflection spectra fine structure to the vibronic interaction connected with Jahn–Teller distortions as well to the core-hole relaxation are discussed.

2. Anisotropic crystal h-BN

Hexagonal BN (h-BN) is one of the most anisotropic layer compounds. The crystalline structure of h-BN is plotted in figure 1. In ordinary conditions h-BN is composed of graphite-like layers, where the atoms of B and N are alternated. In each atomic layer three atoms of N surround each atom of B and vice versa. The theoretical mass density of h-BN is 2.27 g cm^{-3}.

The chemical bonding of h-BN is commonly described by sp^2 hybridization of boron and nitrogen orbitals. This leads to the origin within each layer of trigonal σ bonds with participation of three valence electrons from boron and three from nitrogen. The π orbitals are formed by the overlap of Np_z orbitals containing two p electrons with empty B$2p_z$ orbitals which are perpendicular to layers. The strong anisotropy of chemical bonding along and perpendicular to atomic layers in h-BN results in the sets of π^* and σ^* resonances characterizing the B and N K-shell absorption spectral dependence. According to [5] the π^* are the lowest excitations and the σ^* are the highest ones.

The specific character of crystalline and electronic structure of h-BN leads also to the strong anisotropy in the interaction of h-BN with polarized radiation. Using the dipole approximation, the transition probability of the electron from the core levels to the free states of the conduction

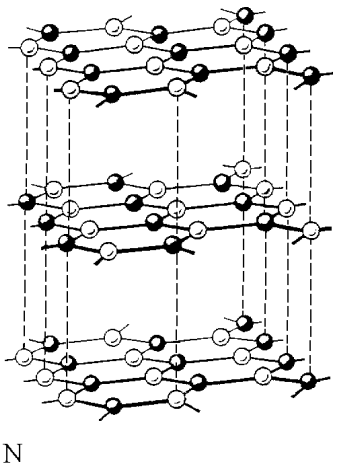

Figure 1. Crystalline structure of h-BN.

band is given by

$$W \approx \left| \int \psi_j^* z \psi_i \, \mathrm{d}\tau \right|^2, \tag{2}$$

where the z axis is parallel to the $\boldsymbol{c}$ axis of the crystal and ψ_i and ψ_j are wavefunctions of the initial and final states, respectively, and $\mathrm{d}\tau$ is a volume element. Because K-shell excitations are viewed, the initial state of the transitions is the 1s level of the B (N) atom, which has a spherical even wavefunction and always is even relative to the reflection in the layer plane. As can be seen from (2) only a transition probability to an odd state is not equal to zero. When $\boldsymbol{E} \perp \boldsymbol{c}$ alignment is realized only transitions to the final states with even wavefunction ψ_j are allowed. So according to the dipole selection rules with regard to the crystal symmetry the absorption in h-BN must originate from transitions from B 1s (N 1s) to σ states in the case $\boldsymbol{E} \perp \boldsymbol{c}$ and from B 1s (N 1s) to π states in the case of $\boldsymbol{E} \parallel \boldsymbol{c}$.

Using polarized radiation one would expect the polarization dependence of the K-shell x-ray reflection near edge structure in h-BN to be a representation of polarization dependence of the absorption spectra. When unpolarized radiation is used and taking into account the cross nature of electromagnetic waves ($\boldsymbol{E} \perp \boldsymbol{q}$, where $\boldsymbol{q}$ is the photon wavevector) one can change the ratio of components $\boldsymbol{E} \perp \boldsymbol{c}$ and $\boldsymbol{E} \parallel \boldsymbol{c}$ by turning the crystal. By means of this rotation, one can change the contributions of different transitions to the B K- (N K-) absorption spectra.

3. Experimental details

The angular spectral dependences of the reflection coefficients were carried out at the synchrotron radiation laboratory HASYLAB at the UHV reflectometer using s-polarized synchrotron radiation and in the special chamber attached to the RSM-500 x-ray spectrometer–monochromator in which the bremsstrahlung from the tungsten anode of the x-ray tube has been used. Details of both experiments were fully considered in [1–3]. Notice that the energy resolution near the B K-absorption edge was 0.7 eV in the experiment with an x-ray tube. In the experiment with s-polarized synchrotron radiation the energy resolution is about $1/200$.

Different orientations of the textured polycrystalline h-BN crystal about the electric field vector $\boldsymbol{E}$ were investigated. They are plotted in figure 2. The reflectivity from two crystal surfaces cut parallel (figure 2, orientation B) and perpendicular (figure 2, orientation A) to

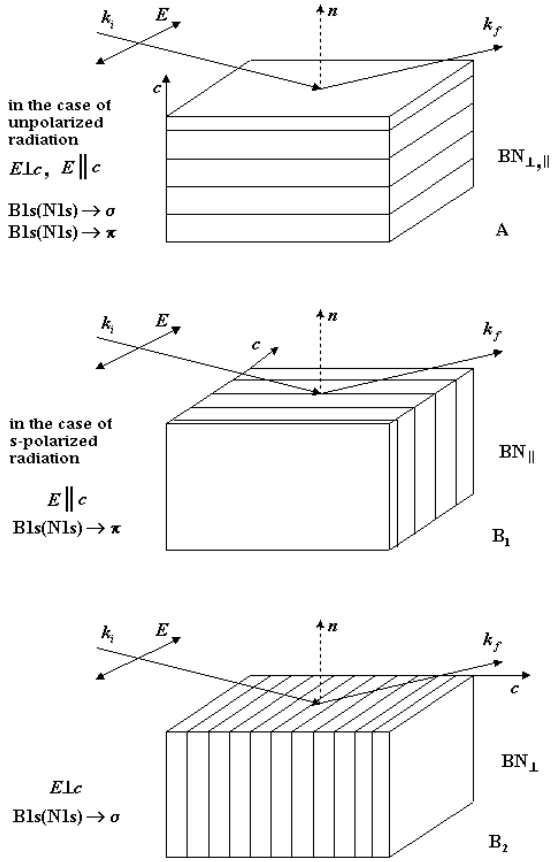

Figure 2. Different orientations of the crystal h-BN about the electric field vector $\boldsymbol{E}$. A, B_1 and B_2 label the crystal orientation.

the $\boldsymbol{c}$ axis of the crystal has been studied experimentally. Moreover, for the same surface cut parallel to the $\boldsymbol{c}$ axis of the crystal but variously oriented with respect to the electric field vector $\boldsymbol{E}$ (figure 2, orientations B_1 and B_2) were analysed too.

When s-polarized radiation is used the absorption spectrum is largely originated from transitions B 1s (N1s) $\rightarrow \pi$ states in the case of the orientation B_1 ($\boldsymbol{E} \parallel \boldsymbol{c}$) and from transitions B 1s (N1s) $\rightarrow \sigma$ states in the case of the orientation B_2 ($\boldsymbol{E} \perp \boldsymbol{c}$). When unpolarized radiation is used the contribution of each component ($\boldsymbol{E} \perp \boldsymbol{c}$ and $\boldsymbol{E} \parallel \boldsymbol{c}$) to the overall reflection process is analysed. For orientation B_2 the electric field vectors are always aligned in the plane parallel to the basal plane and so geometry like $\boldsymbol{E} \perp \boldsymbol{c}$ is realized in this case. For orientation A the vectors $\boldsymbol{E}$ can be arranged within ($\boldsymbol{E} \perp \boldsymbol{c}$) as well as perpendicular ($\boldsymbol{E} \parallel \boldsymbol{c}$) to the basal plane.

4. Results and discussion

4.1. B and N K-reflection spectra of h-BN

Figure 3 shows the B K-reflection spectra obtained for different grazing incidence angles (2.5°, 3°, 4°, 8°) for the crystal orientations B_1 and B_2 using s-polarized radiation. The B K-reflection spectra obtained for crystal orientations A and B_2 using unpolarized radiation are

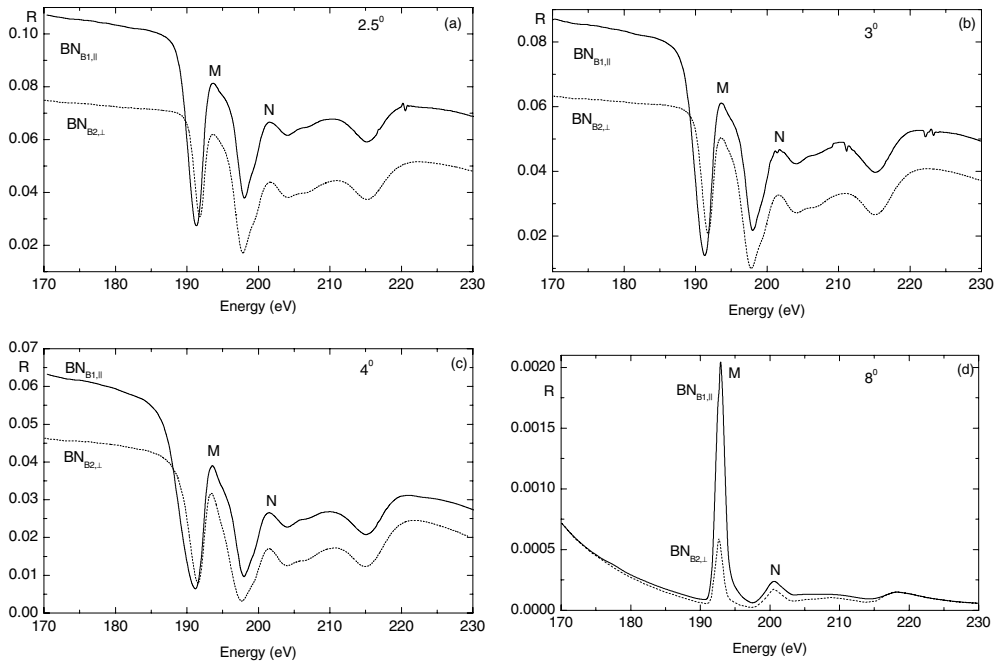

Figure 3. B K-reflection spectra of h-BN obtained for different grazing incidence angles for crystal orientations B_1 and B_2 using s-polarized radiation. The solid curve denotes the data for the orientation B_1 ($BN_{B1,\|}$) and the dotted curve denotes the data for orientation B_2 ($BN_{B2,\perp}$). (a) $\theta = 2.5°$, (b) 3°, (c) 4°, (d) 8°.

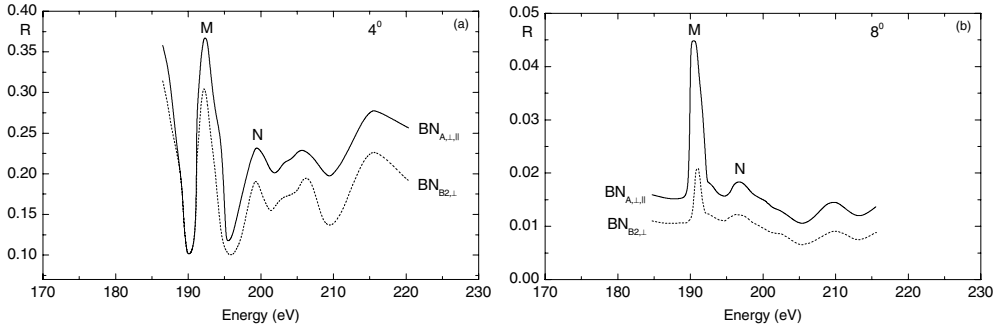

Figure 4. B K-reflection spectra of h-BN obtained for grazing incidence angles 4° and 8° for crystal orientations A and B_2 with use of unpolarized radiation. The solid curve denotes the data for orientation A ($BN_{A,\perp,\|}$) and the dotted curve denotes the data for orientation B_2 ($BN_{B2,\perp}$). (a) $\theta = 4°$, (b) 8°.

plotted in figure 4. Analysis of the reflection spectra fine structure (figures 3, 4) indicates that the reflection spectra for different orientations are similar in the number of essential features and their energy positions for all investigated angles. The shape of the reflection spectra for small incidence angles ($\theta \leqslant 4°$) depends only slightly on the crystal orientation. As this takes place the ratio between magnitudes of peaks M and N is found to be larger for orientation B_1 as compared with orientation B_2 (figure 3) and for orientation A as compared with orientation B_2 (figure 4). The growth of the incidence angle to 8° leads to a significant increase of the

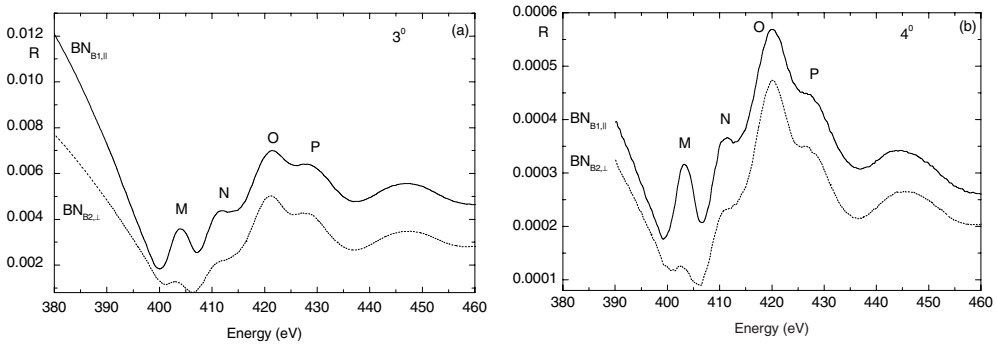

Figure 5. N K-reflection spectra of h-BN obtained for grazing incidence angles 3° and 4° for the crystal orientations B_1 and B_2 using s-polarized radiation. The solid curve denotes the data for orientation B_1 ($BN_{B1,\parallel}$) and the dotted curve denotes the data for orientation B_2 ($BN_{B2,\perp}$). (a) $\theta = 3°$, (b) 4°.

intensity of peak M in the case of orientations B_1 and A. A strong intensity dependence due to crystal orientation exists for peak M for this angle. Recall that exactly in the case of crystal orientations B_1 and A the absorption spectrum is essentially originated from the transitions $B1s \rightarrow \pi$ states.

Figure 5 shows the N K-reflection spectra obtained for grazing incidence angles 3° and 4° for crystal orientations B_1 and B_2. The orientation dependence of feature M in the reflection spectra for both angles has engaged our attention. A higher magnitude of peak M is detected for orientation B_1. In this case transitions $B1s \rightarrow \pi$ states are dominant. The orientation dependence of feature O in the reflection spectra obtained for incidence angle 4° is noteworthy too. A higher magnitude of peak O is observed for orientation B_2. In this case transitions $B1s \rightarrow \sigma$ states are dominant.

The joint examination of B and N K-reflection spectra for different orientations allows definite conclusions. Peak M defines significantly the orientation dependence of B K-reflection spectra. It is the intensity of peak M which is the most sensitive to the changes of the incidence angle and to the crystal orientation. A completely different type of situation occurs in the N K-reflection spectra. In this case all peaks are involved equally in formation of the fine structure. The orientation dependence is described by peaks M and O. Hence the joint analysis of B and N K-reflection spectra points to the different dynamics of the formation of K-reflection spectra near B- and N-edges.

4.2. B and N K-absorption spectra of h-BN

To interpret these effects the absorption spectra were calculated from the reflection spectra by means of Kramers–Kronig relations using the method described in [6]. By way of example figure 6 shows the reflection spectra for both orientations measured in a wide energy region for the incidence angle 4°. In the strict sense the applicability of Kramers–Kronig analysis to the anisotropic crystal is not evident. The main problem in this case is connected with taking into account the surface roughness. Because of the composite micro-structure the surface of any crystal side (cut parallel or perpendicular to the $\boldsymbol{c}$ axis) will be disrupted by splits after any type of technological polishing. So a prerequisite for the formation of scattering into the substance, in addition to scattering into vacuum, is produced. Up until now no theoretical description of the scattering deep into the material has been available. This is the reason that

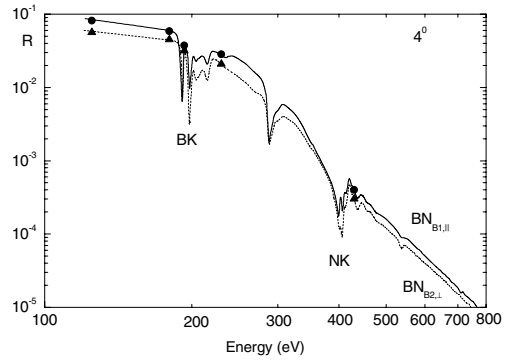

Figure 6. Reflection spectra of h-BN obtained for grazing incidence angle 4° for crystal orientations B_1 and B_2 using s-polarized radiation in a wide energy region. The solid curve denotes the data for orientation B_1 ($BN_{B1,\|}$) and the dotted curve denotes the data for orientation B_2 ($BN_{B2,\perp}$).

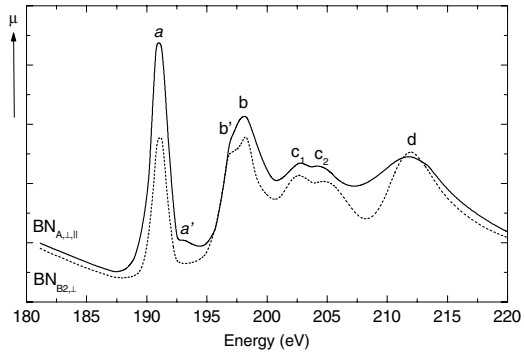

Figure 7. B K-absorption spectra of h-BN calculated from reflection spectra obtained for grazing incidence angle 4° for crystal orientations A and B_2 using unpolarized radiation. The solid curve denotes the data for orientation A ($BN_{A,\perp,\|}$) and the dotted curve denotes the data for orientation B_2 ($BN_{B2,\perp}$).

the surface roughness was not taken into account in the calculations of the absorption spectra. According to a large body of research the relative differences in the calculated spectra will be correct.

The calculated B K-absorption spectra are plotted in figures 7 and 8. One can see that the spectra obtained by the use of s-polarized synchrotron radiation and unpolarized radiation have similar numbers of features and similar energy dependences. Notice that more clearly defined features (a', b', c_1 and c_2) are found in the spectra obtained using the unpolarized radiation (figure 7). The reason is a higher energy resolution in the experiment using the x-ray tube.

Analysis of the calculated B K-absorption spectra shows that the energy position of all features is independent of the crystal orientation and the incidence angle that was used in the calculations whereas the intensity of all features depends on the crystal orientation. One can see that the selective line a dominates in the calculated B K-absorption spectra. The intensity of this peak is larger in the spectra obtained for the crystal orientation when $\boldsymbol{E} \parallel \boldsymbol{c}$ (figure 2, orientation B_1). In this case transitions B1s $\rightarrow \pi$ states are dominant. When using unpolarized radiation the value of selective absorption in peak a is larger in the spectrum obtained for orientation A (figure 2) for which the electric field vector $\boldsymbol{E}$ can be arranged

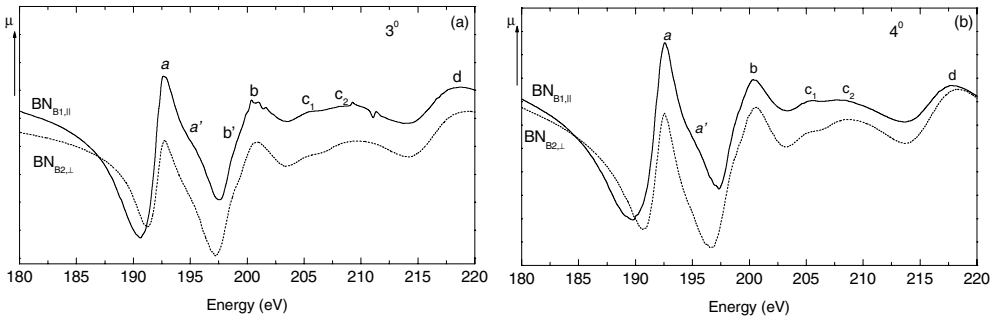

Figure 8. B K-absorption spectra of h-BN calculated from reflection spectra obtained for grazing incidence angles 3° and 4° for crystal orientations B_1 and B_2 using s-polarized radiation. The solid curve denotes the data for the orientation B_1 ($BN_{B1,\parallel}$) and the dotted curve denotes the data for orientation B_2 ($BN_{B2,\perp}$). (a) $\theta = 3°$, (b) 4°.

both within and perpendicular to the basal plane. The intensity of features b, c, d is larger for the crystal orientation when the alignment $\boldsymbol{E} \perp \boldsymbol{c}$ is realized (figure 2, B_2) and transitions $1s \rightarrow \sigma$ states are dominant in this case.

The dynamics of the orientation and angular dependences of the calculated B K-absorption near edge structure correlates well with the calculations carried out in the framework of the quasi-atomic approach in the work [7]. According to [7] the B K-excitations are essentially localized within the nearest neighbours (within a planar BN_3^{6-} fragment). The π interaction within a basal (xy) plane as well as between the neighbouring layers can be neglected in this case. Feature a is assigned to the single B $1s^{-1}\ 2p_z a_2''$ resonance and can be ascribed to a transition from the B 1s level to the atom-like (practically non-bonding) π MO. Feature b is assigned to the double degenerate B $1s^{-1}\ e'(2p_{xy})$ resonance and can be ascribed to transitions into localized two-centre σ^* MOs. Essentially, the $2p_z a_2''$-splitting component is oriented normally to the basal plane and the $e'(2p_{xy})$-splitting component is located within a basal plane.

The dynamics of the orientation dependence of feature c in the calculated spectra supports the assumption that this feature connects with the transitions to the $2\sigma^*$ state [7]. The origin of feature d is unknown. According to our investigations the intensity of this peak increases for the crystal orientation when $\boldsymbol{E} \perp \boldsymbol{c}$ is valid.

One can see that feature b (σ^* resonance) has double structure in all calculated B K-absorption spectra (figures 7 and 8). It is significant that the much clearer resolution of this structure (b, b') is observed in the spectra corresponding to the crystal orientation when $\boldsymbol{E} \perp \boldsymbol{c}$, that is the transitions to σ states (localized within the basal plane) become dominant. The appearance of the doublet structure for the σ^* resonance in the absorption near edge structure of plane molecules and plane coordinated atoms in complex ions is a situation often observed and usually connected with Jahn–Teller distortions [8–12].

The average splitting value $\Delta_{\pi\sigma} = 0.5(\Delta_{\pi\sigma_1} + \Delta_{\pi\sigma_2})$ for the σ^* resonance maxima in the B K-absorption spectra that were calculated from the reflection spectra obtained using an x-ray tube (figure 7) is equal to 6.73 eV. As this value correlates well with the dependence of the energy splitting $\Delta\pi\sigma$ on the interatomic distance for K excitations in planar $[BX_3]^{n-}$ fragments and free BF_3, BCl_3 and BBr_3 molecules and taking into account the orientation dependence that was discovered, the Jahn–Teller mechanism seems to be plausible for the explanation of the appearance of the observed doublet structure. In other words, the doublet structure of feature b can be correlated with the additional splitting of the doubly degenerate

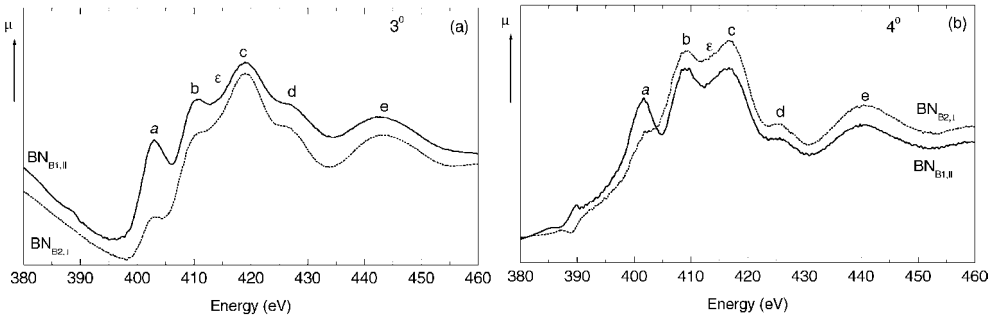

Figure 9. N K-absorption spectra of h-BN calculated from reflection spectra obtained for grazing incidence angles 3° and 4° for crystal orientations B_1 and B_2 using s-polarized radiation. The solid curve denotes the data for orientation B_1 ($BN_{B1,\parallel}$) and the dotted curve denotes the data for orientation B_2 ($BN_{B2,\perp}$). (a) $\theta = 3°$, (b) 4°.

e' ($2p_{xy}$) excitation due to low symmetry distortions of the nearest environment. Notice that the obtained energy splitting $\Delta\pi\sigma$ agrees well with the value $\Delta\pi\sigma = 6.75$ eV taken from the B K-absorption spectrum measured for h-BN in [7].

Now we would like to consider shoulder a' which emerges in the vicinity (upward shift ≈2 eV) of selective peak a. Analysis of the orientation dependences shows that shoulder a' is only manifested in the B K-absorption spectra calculated from the reflection spectra obtained in the geometry when transitions B1s $\rightarrow \pi$ states are dominant (orientations B_1 and A, figure 2); that is, the origin of shoulder a' connects with the transitions to π^* states. At the same time because peak a is assigned to the single B $1s^{-1}$ $2p_z a_2''$ resonance shoulder a' cannot be assigned to a single-electron transition. According to [7, 13] π-resonance in h-BN can be presented as a sum over the B $1s^{-1}$ $2p\pi$-excitations localized in the planar and pyramidal [B* N_3] configurations induced by the relaxation near the core-excited atom. For the pyramidal C_{3v} configuration the local atomic deformation takes place. Such a configuration is achieved when the nitrogen atoms are fixed at their regular positions and the π-core-excited B atom is an out-of-plane displacement (of ≈0.16 Å) of the core-excited atom resulting in defect boron sites in the crystal. The appearance of the pyramidal metastable configuration has been made possible by the promotion of a core-level electron into unoccupied molecular orbitals. According to [13] for the C_{3v} configuration, the a' MO becomes antibonding (π^*) owing to the strong interaction of the B $2p_z$ with the N $2p_z$ and 3s functions; an upward shift of the π^*-resonance energy relative to the π-resonance energy is expected.

Notice that the analogous feature shifted to the range of large energies of ≈2.1 eV was identified in the orientation dependences of the C K-electron energy loss spectra in graphite in [14]. According to [14, 15], the origin of this feature is core-hole relaxation too.

It must be emphasized that it has been investigation of the orientation dependences in both experiments (with h-BN and graphite) which has led to the understanding of the origin of shoulder a'.

Figure 9 shows N K-absorption spectra calculated from the reflection data. These spectra demonstrate clearly the orientation dependence that was established during the analysis of the B K-absorption spectra, that is the intensity of peak a is greater for the geometry $\boldsymbol{E} \parallel \boldsymbol{c}$, and the intensities of peaks b and c are larger for the geometry $\boldsymbol{E} \perp \boldsymbol{c}$. One can see that there is a clearer orientation dependence for feature a in N K-absorption spectra too, but in this case feature a is not dominant in the spectra. The N K-absorption spectrum demonstrates three intense absorption lines (a, b, c) and two broad absorption bands (d and e).

The surprising thing is that the dependence of the energy position of all features and the incidence angle takes place in this case. The spectra $\mu_{4^\circ}(E)$ are shifted downward with respect to the spectra $\mu_{3^\circ}(E)$ by $\approx$2 eV. As this takes place the energy distance between peaks *a* and *b* is conserved and that between peaks *b* and *c* is decreased in spectra for both orientations. The growth of the incidence angle leads to an intensity redistribution between peaks *b* and *c* especially in the case of crystal orientation B_2. All of these have verified the theoretical prediction that the interpretation of the N K-absorption spectra taking into account only the nearest neighbours is not sufficient, as in the case of the B K-absorption spectra. The resonance effects inside surroundings (REIS), i.e. inside the nearest and next nearest coordination shells, dominate in this case. Just the second coordination shell formed by six atoms of N exerts a noticeable influence on the σ^* excitations while the effects of the third and other distant shells on the $\mu(E)$ are weak. According to [7], peak *a* can be assigned to $\pi^*(\mathrm{N1s^{-1}2p_z}a_2'')$ and peaks *b* and *c* to the first and the second $\sigma * (\mathrm{N1s^{-1}}e'(\mathrm{2p}_{xy}))$ resonances, respectively.

Analysing the energy dependence of the photoelectron reflection coefficients for one and two coordination shells of the core ionized N atom in h-BN the authors of [7] show that, due to the REIS, the 'window' of transparency and two abnormal reflection regions (one region before and another one after the 'window' of transparency) appear in h-BN near the N absorption edge. According to these calculations both σ^* resonances (features *b* and *c*) are located in the regions of abnormal reflection and shoulder ε falls into the 'window' of transparency. Analysis of the angular and orientation dependences of the absorption spectra (figure 9) testifies to the fact that with the growth of the incidence angle the energy position of shoulder ε remains the same but the energy distance Δ_{b-c} between peaks *b* and *c* falls from 8.8 to 7.4 eV. Notice that the calculated value in [7] is $\Delta_{b-c} = 10.04$ eV, and the meaning $\Delta_{b-c} = 7.5$ eV was obtained in [7] from the experimental absorption spectrum. Because the surroundings as an indivisible subsystem act on atomic excitations motivating the appearance of peaks *b* and *c* these peaks connect with a peculiarities of the electronic structure. So, it would appear reasonable that the change of Δ_{b-c} is caused by variations in the crystalline structure. Really the change of the incidence grazing angle leads to the change of the depth of formation of the reflected beam. According to [16] the technological treatment of the sample surface produces a mechanically destroyed surface layer. An increase in the incidence grazing angle leads to greater probing depth and hence participation of more perfect layers in forming the reflected radiation beam.

Summarizing, one can conclude a noticeable difference between B and N π^* excitations which evidences that the $2p_z$ state of N dominates the π interaction along an atomic layer while the B states stay atom-like because of their strong spatial localization. Analysis of the orientation dependences of the x-ray reflectivity near both edges strongly supports the possibility of tracing the role of each excitation canal in the formation of fine structure.

4.3. Remarks

According to figure 3 B K-reflection spectra for different crystal orientations of the same surface at small incidence angles are very similar but differ significantly in absolute values of the reflection coefficients. The reflection coefficients for orientation B_1 are approximately 1.5-fold greater than for orientation B_2 at all energies. Figure 10 shows angular dependences of the reflection coefficient and angular distributions of scattered radiation for a grazing incidence angle $\theta = 8^\circ$ from crystal orientations B_1 and B_2 obtained at the energies $E = 180$ eV (range of normal dispersion) and $E = 193$ eV (in the region of π resonance). As can be seen the reflectivity for face B_1 is larger than for face B_2 in the region of normal dispersion ($E = 180$ eV). The integral scattering intensities from both faces are similar in shape, but in the case of crystal orientation B_2 it is larger. Because the same surface was investigated in

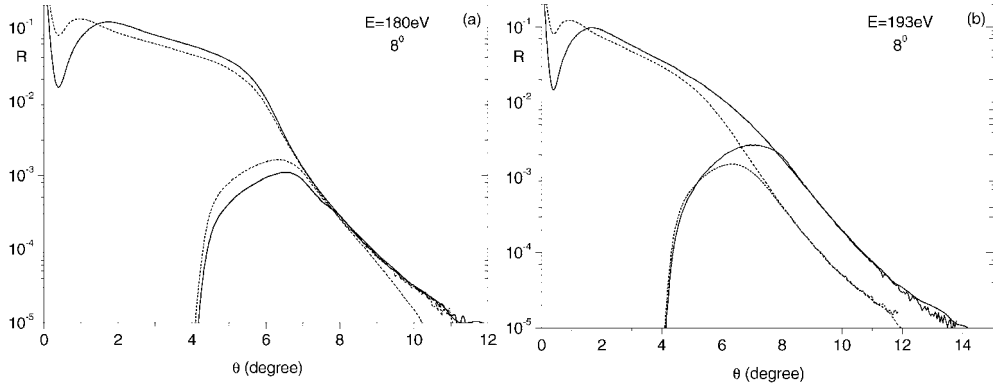

Figure 10. Angular dependences of the reflection coefficient and angular distribution of scattered radiation obtained for grazing incidence angle 8° for crystal orientations B_1 and B_2 using s-polarized radiation. The solid curve denotes the data for orientation B_1 ($BN_{B1,\parallel}$) and the dotted curve denotes the data for orientation B_2 ($BN_{B2,\perp}$). Energy: (a) $E = 180$ eV, (b) $E = 193$ eV.

both cases it would appear reasonable that the revealed distinction connects with the planar anisotropy of the surface.

A different situation arises with the energy $E = 193$ eV. In this case the reflectivity and integral scattering intensity both are larger for the crystal orientation B_1. Moreover the difference in anomalous scattering peak positions for the crystal orientations B_1 and B_2 should be noted. The difference measures 1°. Taking into account the connection of the angular position of the anomalous scattering peak with the critical angle of total external reflection (anomalous scattering peak angular position coincides with critical angle [17]) it is reasonably safe to suggest that the critical angles for crystal orientations B_1 and B_2 in the region of π resonance are distinguished on 1°.

5. Conclusions

The experimental investigation of the spatial crystal anisotropy effect of h-BN on the x-ray reflection using both s-polarized synchrotron radiation and unpolarized radiation have been carried out. It has been found that a very strong orientation dependence of the reflection and calculated absorption spectra near both B- and N K-absorption edges on crystal orientation with respect to the electric field vector $\boldsymbol{E}$ exists in this case: when a strong anisotropy of chemical bonding along and perpendicular to atomic layers results in the sets of π and σ resonances characterizing the B and N K-shell absorption spectral dependence.

The principle of this dependence consists in varying degrees of a manifestation of the transitions of 1s electrons to π ($2p_z a_2''$-component) and to σ ($e'(2p_{xy})$-component) states of the conduction band in relation to the crystal orientation which is defined by the relative positions of the electric field vector $\boldsymbol{E}$ and the crystal axis $\boldsymbol{c}$ ($\boldsymbol{E} \parallel \boldsymbol{c}$ or $\boldsymbol{E} \perp \boldsymbol{c}$). The joint analysis of B and N K-reflection and calculated absorption spectra points to the different dynamics of the formation of K-spectra near B and N edges. It has been just the angular dependences of the reflection spectra which have clearly demonstrated the theoretical prediction that the interpretation of the N K-absorption spectra taking into account only the nearest neighbours is not sufficient, as it was in the case of the B K-absorption spectra. Analysis of the reflection spectra (and calculated absorption data) obtained in the conditions of a higher energy resolution shows a high sensitivity of the reflection spectra fine structure to the vibronic interaction connected

with Jahn–Teller distortions as well to the core-hole relaxation. A very strong dependence of the absolute values of the reflectivity on planar crystal anisotropy was discovered.

The investigation submitted provides strong evidence that the use of x-ray spectroscopy of reflection and scattering opens additional possibilities for study of the anisotropic crystals. It should be realized that the data submitted in this work are the first step in the comprehension of the origin of the spatial crystal anisotropy effect on the x-ray reflection and scattering. Further experimental investigations of more composite materials are required.

References

[1] Filatova E O and Blagoveshenskaya T A 1993 *J. X-Ray Sci. Technol.* **4** 1
[2] Filatova E O, Pavlychev A A, Blessing C and Friedrich J 1995 *Physica* B **208/209** 417
[3] Filatova E O, Stepanov A P, Blessing C, Friedrich J, Barchewitz R, Andre J-M, Le Guern F, Bac S and Troussel D 1995 *J. Phys.: Condens. Matter* **7** 2731
[4] Vedrinskii R V, Kraizman V L, Novakovich A A and Machavariani V Sh 1992 *J. Phys.: Condens. Matter* **4** 6155
[5] Nakhmanson M S and Smirnov V P 1971 *Fiz. Tverd. Tela* **13** 3288 (Engl. transl. 1972 *Sov. Phys.–Solid State* **13** 2763)
[6] Filatova E, Lukyanov V, Barchewitz R, Andre J-M, Idir M and Stemmler Ph 1999 *J. Phys.: Condens. Matter* **11** 3355
[7] Franke R, Bender S, Hormes J, Pavlychev A A and Fominych N G 1997 *Chem. Phys.* **216** 243
[8] Nekipelov S V, Akimov V N and Vinogradov A S 1988 *Sov. Solid State Phys.* **30** 3647
[9] Nekipelov S V, Akimov V N and Vinogradov A S 1991 *Sov. Solid State Phys.* **33** 663
[10] Franke R, Bender St and Hormes J 1995 *Physica* B **208/209** 293
[11] Ishiguro E, Iwata S, Suzuki Y, Mikuni A and Sasaki T 1982 *J. Phys. B: At. Mol. Phys.* **15** 1841
[12] Ma Y, Skyt P, Wassdahl N, Glans P, Manchini D C, Guo J and Nordgren J 1993 *Phys. Rev. Lett.* **71** 3725
[13] Pavlychev A A, Franke R, Bender St and Hormes J 1998 *J. Phys.: Condens. Matter* **10** 2181
[14] Cheung T T P 1985 *Phys. Rev.* B **31** 4792
[15] Painter G S and Ellis D E 1980 *Phys. Rev.* B **1** 4747
[16] Filatova E O and Shulakov A S 1995 *J. Colloid Interface Sci.* **169** 361
[17] Filatova E O and Blagoveshenskaya T A 1992 *J. X-Ray Sci. Technol.* **3** 204